Cell. Mol. Life Sci. 66 (2009) 1800 – 1816
1420-682X/09/111800-17
DOI 10.1007/s00018-009-9149-8

Cellular and Molecular Life Sciences

Protein kinase CK2: From structures to insights

K. Niefind[a, *], J. Raaf[a] and O.-G. Issinger[b]

[a] Universität zu Köln, Department für Chemie, Institut für Biochemie, Zülpicher Straße 47, 50674 Köln (Germany), Fax: +49 221 4705067, e-mail: Karsten.Niefind@uni-koeln.de
[b] Syddansk Universitet, Institut for Biokemi og Molekylær Biologi, Campusvej 55, 5230 Odense (Denmark)

Online First 24 April 2009

Abstract. Within the last decade, 40 crystal structures corresponding to protein kinase CK2 (former name 'casein kinase 2'), to its catalytic subunit CK2α and to its regulatory subunit CK2β were published. Together they provide a valuable, yet by far not complete basis to rationalize the biochemical features of the enzyme, such as its constitutive activity, acidophilic substrate specificity, dual-cosubstrate specificity and its hetero-tetrameric quarternary structure. Comprehensive sets of structural superimpositions reveal that both CK2α and CK2β are relatively rigid molecules. In CK2β the critical region of CK2α recruitment is pre-formed in the unbound state. In CK2α the activation segment – a key element of protein kinase regulation – adapts invariably the typical conformation of the active enzymes. Recent structures of human CK2α revealed a surprising plasticity in the ATP-binding region, suggesting an alternative mode of activity control. (Part of a Multi-author Review)

Keywords. Protein kinase CK2, casein kinase 2, X-ray crystallography, structural biology, structural plasticity, structural basis of constitutive activity, structural basis of dual-cosubstrate specificity, inactive conformation.

Introduction

The structural biology of protein kinase CK2 began in 1991 with the crystal structure of cAMP-dependent protein kinase (CAPK) [1], which was the first 3D structure of a member of the eukaryotic protein kinase (EPK) superfamily [2] to be published. This structure inspired researchers to regard CK2 from a 3D perspective, leading to the construction of homology models [3], the structure-based design of relevant mutants [4, 5] and the formulation of hypotheses with a structural background. This structural approach received a solid basis a decade ago with the crystallographic analyses of the three main CK2 entities – the catalytic subunit CK2α [6] (Fig. 1A, B), the regulatory subunit CK2β [7] (Fig. 1C, D) and the heterotetrameric complex of both these components in the CK2 holoenzyme [8] (Fig. 1E).

From a global view, the CK2α structure contained all the features that one would expect to find based on the already known structures of CAPK [1], cyclin-dependent kinase 2 (CDK2) [11–13] and some other EPK enzymes. The CK2α molecule is made up of a catalytic core composed of two major folding domains (Fig. 1A) harbouring the active site in between. The N-terminal domain is the smaller one and belongs to the (α+β)-type of folding domains. Its constituting element is an antiparallel β-sheet composed of five β-strands. It is accompanied by a single, long α-helix located next to the inter-domain cleft (helix αC, Fig. 1A, B) which is required for function rather than for structural reasons.

Concerning its principle architecture the C-terminal domain of CK2α is conversely constructed compared to the N-terminal domain: it has an α-helical fold, but at the interdomain region it contains two small, but functionally important, two-stranded β-sheets (β7/β8 and β6/β9, Fig. 1A, B). Most helices within the C-terminal domain are conserved among the EPKs with the exception of the small helices αH, αI and αJ (Fig. 1A), which constitute an insertion that is absent in CAPK but which is typical for the CMGC-family of EPKs [14]. This 'CMGC insert' thus unambiguously

* Corresponding author.

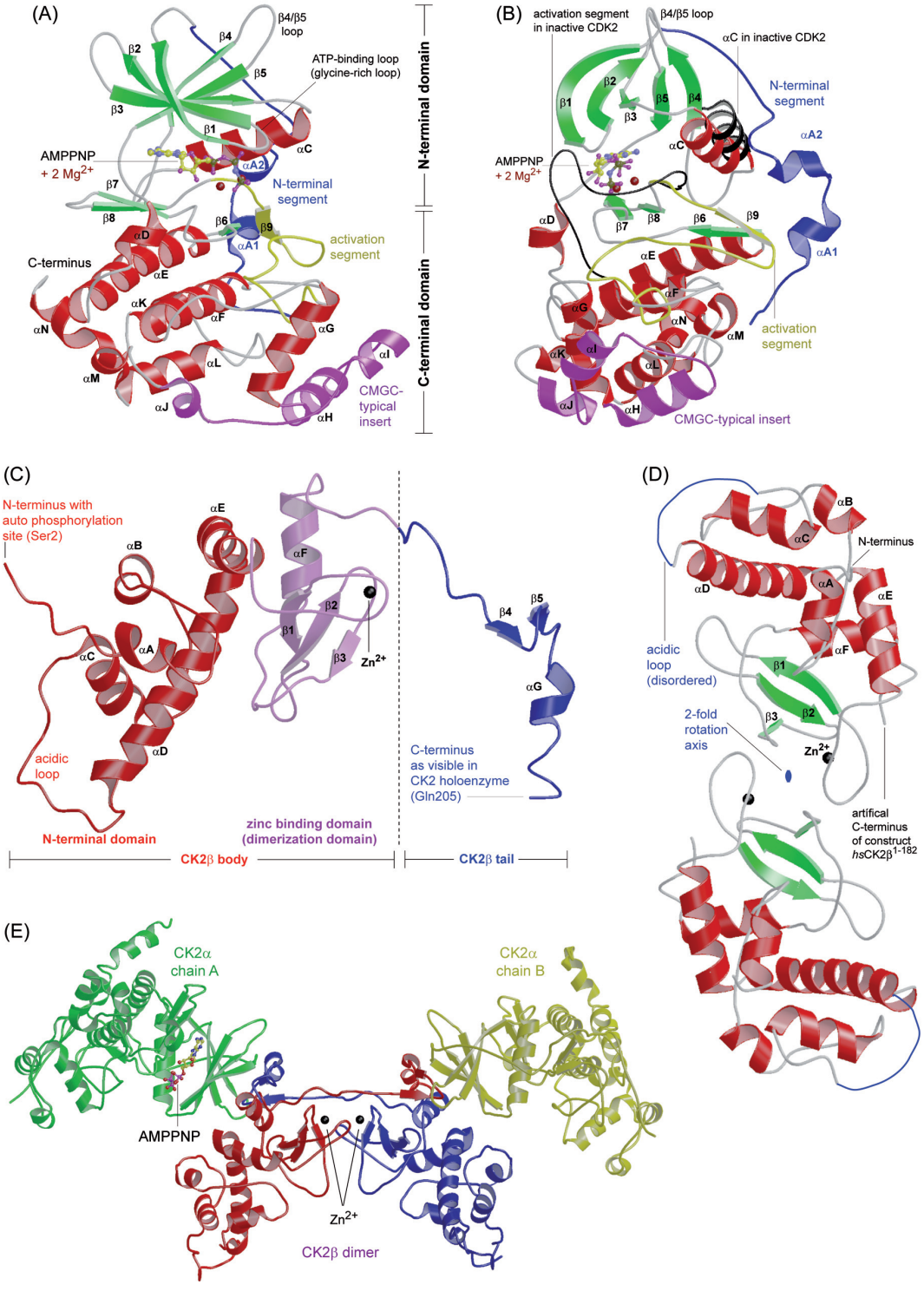

Figure 1. Overview of key structures of protein kinase CK2. (*A*) Catalytic subunit CK2α from *Zea mays* in complex with AMPPNP and magnesium ions [32, 33] drawn in a typical perspective introduced for the first time for CAPK [1]. (*B*) The same as in (*A*) but turned by 90° around a vertical axis so that the interaction of the N-terminal segment (blue) to the typical key regulatory elements of EPKs – the activation segment (yellow) and the helix αC – can be perceived. To indicate a possible inactive conformation of these elements they are drawn in black colour, as found in inactive CDK2 [11]. (*C*) Architecture of a CK2β subunit extracted from the structure of the human CK2 holoenzyme [8]. The two main domains and the extended C-terminal tail, which nestles up against the second CK2β subunit (see panel e of this figure), are indicated by different colours. (*D*) Structure of dimeric *hs*CK2β$^{1-182}$ [7] – the first structure of a CK2β construct and the first experimental confirmation of a zinc-finger motif. (*E*) First and so far only structure of a CK2 holoenzyme complex [8]. All pictures were drawn with BOBSCRIPT [9] and Raster3D [10].

identifies CK2α as a close relative of the eponymous members of the CMGC family, which include the cyclin-dependent kinases (CDKs), the mitogen-activated protein kinases (MAPKs) and glycogen-synthase kinase 3 (GSK3).

Almost no inferences could be made for the first CK2β structure [7], due to the lack of proteins with related amino acid sequences, not to mention 3D structures. Hence the central discovery of this structure – a zinc finger (Fig. 4A) serving as a dimerization motif and resembling a region of the transcription elongation factor TFIIS [15] – came as a surprise. Apart from this local similarity, the global structure of CK2β revealed a novel fold [7]. As in CK2α, the CK2β monomer (Fig. 1C) consists of a core of two domains (later called the 'CK2β body' in the context of the CK2 holoenzyme [8]); yet, in this case, the N-terminal region constitutes the larger domain and belongs to the α-helical folding type. This domain is followed by a smaller one which contains a β-sheet and harbours the zinc-binding site. The first CK2β crystal structure [7] lacked the C-terminal 33 amino acids, which contain the main CK2α interaction motif. This missing information was provided by the third of the early key structures, the CK2 holoenzyme structure (Fig. 1E) [8]. This structure revealed a tail in the CK2β monomer (Fig. 1C) that crosses the CK2β dimer interface to nestle up against both the second CK2β monomer and the CK2α subunit (Fig. 1E). The CK2 holoenzyme structure integrated the previous knowledge about the location of the α/β interface on CK2α [16] and on CK2β [17]. Moreover, the structure confirmed the already established structural role of the CK2β dimer as the constituting center of the holoenzyme, to which the two CK2α subunits attach separately and without contacting each other (Fig. 1E).

Quantity and quality of CK2 structures

At the end of 2008, 40 crystal structures of CK2 entities were available from the Protein Data Bank (PDB) [18] (Table 1). Nearly half of them were accompanied by the corresponding structure factor amplitudes (experimental X-ray diffraction data). The latter allow the calculation of electron densities and thus a critical inspection or even a re-refinement of the respective structure. Like all protein crystal structures, the CK2 structures contain regions of disorder, anomalies and local errors [19]. Modern crystallography programs like COOT [20] enable non-expert users to identify and partly even remove such ambiguities, provided that the experimental diffraction data are available. In the future the novel quality-focussed PDB deposition policy [21] ensures that any new CK2 structure will comprise both atomic coordinates and diffraction data; the use of both of them is strongly recommended [22].

Particular advances in the growth curve of CK2 structures (Fig. 2) can be identified in the years 2002 and 2007, when several CK2α structures with ATP-competitive inhibitors were published, reflecting a general tendency in protein kinase structure research. Meanwhile CK2 is regarded as 'druggable' kinase [23, 24], and companies involved in drug design efforts began to contribute to the structural knowledge about CK2 [25]; thus, it can be assumed that many more CK2α/inhibitor structures have been solved, albeit not published.

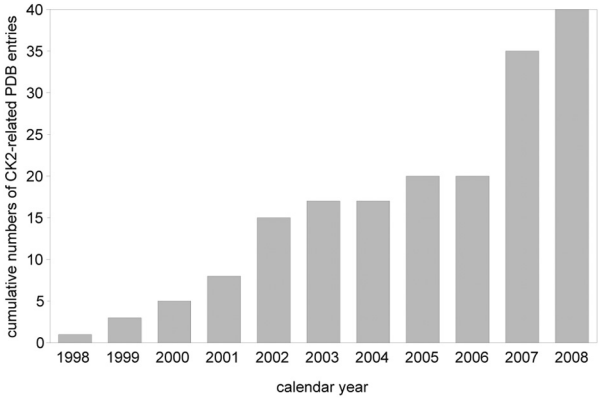

Figure 2. Growth of the knowledge about CK2 structures. The histogram indicates the cumulative numbers of CK2-related structures deposited in the PDB [18].

While the structural information about CK2α-bound small molecules is rapidly growing, an inspection of Table 1 reveals its limitations concerning the protein matrices. Although CK2 subunits are encoded in all (CK2α) or almost all (CK2β) eukaryotic genomes known today – often in several isoforms – the predominant majority of CK2 structures refers to one particular entity, i.e. CK2α, to two species, i.e. *Zea mays* and *Homo sapiens*, and to only one paralog within these species. In particular the CK2 holoenzyme is represented only by the above-mentioned low-resolution structure [8].

Technical and functional reference structures

A further limitation of the CK2 structures concerns a technical aspect: all but one CK2 structure (Table 1) were solved using the molecular replacement method [26] in which an already known similar structure is used as a starting model. This leads to the so-called 'model bias' [26], which means that the final structure preserves to a certain degree – depending on the resolution, the

Table 1. CK2 structures available at the Protein Data Bank [17] ranked according to resolution.

Protein construct/ designation in the text	Species	Main ligands	Resol. [Å]	Exp. data available?	PDB code	Ref.
*hs*CK2α$^{1-335}$	*H. sapiens*	3-methyl-1,6,8-trihydroxyanthraquinone (emodin)	1.50	yes	3BQC	[33]
*hs*CK2α$^{1-335}$	*H. sapiens*	5,6-dichloro-1-β-D-ribofuranosyl-1H-benzimidazole (DRB)	1.56	yes	3H30	[29]
*hs*CK2α$^{1-335}$	*H. sapiens*	adenosine 5′-(β,γ-imido)triphosphate (AMPPNP), sulphate ions	1.61	yes	2PVR	[34]
*hs*CK2α$^{1-335}$V66A/M163L	*H. sapiens*	adenosine 5′-(β,γ-imido)triphosphate (AMPPNP), glycerol	1.66	yes	3BW5	[29, 31]
*zm*CK2α	*Zea mays*	[5-oxo-5,6-dihydroindolo-(1,2-a)quinazolin-7-yl]-acetic acid	1.68	no	1OM1	[35]
*zm*CK2α	*Zea mays*	5,8-diamino-1,4-dihydroxyanthrachinon	1.70	no	1M2R	[36]
*zm*CK2α	*Zea mays*	2-(cyclohexylmethylamino)-4-(phenylamino)pyrazolo[1,5- a][1,3,5]triazine-8-carbonitrile	1.70	no	2PVJ	[24]
*hs*CK2β$^{1-182}$	*H. sapiens*	–	1.74	no	1QF8	[7]
*zm*CK2α	*Zea mays*	4,5,6,7-tetrabromo-N,N-dimethyl-1H-benzimidazol-2-amine	1.77	no	1ZOE	[37]
*zm*CK2α	*Zea mays*	1,8-dihydroxy-4-nitro-xanthen-9-one	1.79	no	1M2Q	[36]
*zm*CK2α	*Zea mays*	4,5,6,7-tetrabromo-benzimidazole	1.81	no	2OXY	[38]
*zm*CK2α	*Zea mays*	5,6,7,8-tetrabromo-1-methyl-2,3-dihydro-1H-imidazo[1,2-a]benzimidazole	1.81	no	1ZOH	[37]
*zm*CK2α	*Zea mays*	3,8-dibromo-7-hydroxy-4-mmethyl-2H-chromen-2-one	1.85	yes	2QC6	[39]
*zm*CK2α	*Zea mays*	probably benzamidine	1.86	yes	1LPU	[31]
*zm*CK2α	*Zea mays*	adenosine 5′-(β,γ-imido)triphosphate (AMPPNP)	1.86	yes	1LP4	[31]
*zm*CK2α	*Zea mays*	2-(4-ethylpiperazin-1-yl)-4-(phenylamino) pyrazolo[1,5-a][1,3,5] triazine-8-carbonitrile	1.90	no	2PVL	[24]
*zm*CK2α	*Zea mays*	2-(4-chlorobenzylamino)-4-(phenylamino) pyrazolo[1,5-a][1,3,5]triazine-8-carbonitrile	1.90	no	2PVK	[24]
*hs*CK2α$^{1-335}$	*H. sapiens*	3-methyl-1,6,8-trihydroxyanthraquinone (emodin)	1.95	yes	3C13	[33]
*zm*CK2α	*Zea mays*	probably benzamidine	2.00	yes	1LR4	[33]
*zm*CK2α	*Zea mays*	1,8-dihydroxy-4-nitro-anthrachinon	2.00	no	1M2P	[36]
*zm*CK2α	*Zea mays*	N-(3-(8-cyano-4-(phenylamino)pyrazolo[1,5-a][1,3,5]triazin-2-ylamino) phenyl)acetamide	2.00	no	2PVN	[24]
*zm*CK2α	*Zea mays*	4-(2-(1H-imidazol-4-yl)ethylamino)-2-(phenylamino) pyrazolo[1,5-a][1,3,5]triazine-8-carbonitrile	2.00	no	2PVM	[24]
*zm*CK2α	*Zea mays*	–	2.18	no	1JAM	[40]
*zm*CK2α	*Zea mays*	4,5,6,7-tetrabromo-2-benzotriazole	2.19	no	1J91	[40]
*zm*CK2α	*Zea mays*	adenosine 5′-(β,γ-imido)triphosphate (AMPPNP)	2.20	yes	1DAW	[31]
*zm*CK2α	*Zea mays*	guanosine 5′-(β,γ-imido)triphosphate (GMPPNP)	2.20	yes	1DAY	[31]
*zm*CK2α	*Zea mays*	N,N′-diphenylpyrazolo[1,5-a][1,3,5]triazine-2,4-diamine	2.20	no	2PVH	[24]
*hs*CK2α$^{1-335}$	*H.sapiens*	glycerol	2.30	yes	3FWQ	[41]
*zm*CK2α	*Zea mays*	4,5,6,7-tetrabromo-1H,3H-benzimidazole-2-one	2.30	no	1OXD	[38]
*zm*CK2α	*Zea mays*	4,5,6,7-tetrabromo-1H,3H-benzimidazole-2-thion	2.30	no	2OXX	[38]
*zm*CK2α	*Zea mays*	4,5,6,7-tetrabromo-2-(methylsulphanyl)-1H-benzimidazole	2.30	no	1ZOG	[37]
*hs*CK2α$^{1-329}$E27A/K76N*	*H. sapiens*	–	2.40	yes	1NA7	[42]
*hs*CK2α$^{1-335}$	*H. sapiens*	adenosine 5′-(β,γ-imido)triphosphate (AMPPNP)	2.50	yes	1PJK	[43]
*zm*CK2α	*Zea mays*	3-methyl-1,6,8-trihydroxyanthraquinone	2.63	no	1F0Q	[44]
*hs*CK2β$^{1-193}$	*H. sapiens*	–	2.80	yes	3EED	[26]
*xl*CK2β$^{1-178}$	*X. laevis*	p21WAF1 peptide	2.89	yes	1RQF	[45]
*rn*CK2α$^{1-335}$	*R. norvegicus*	sulphate ions	3.00	yes	2R7I	–
(*hs*CK2α$^{1-337}$)$_2$/ (*hs*CK2β)$_2$*	*H. sapiens*	adenosine 5′-(β,γ-imido)triphosphate (AMPPNP)	3.10	yes	1JWH	[8]

Table 1 *(Continued)*

Protein construct/ designation in the text	Species	Main ligands	Resol. [Å]	Exp. data available?	PDB code	Ref.
*rn*CK2β$^{1-193}$ *	*R. norvegicus*	–	3.10	yes	2R6M	–
*zm*CK2α	*Zea mays*	adenosine monophosphate (AMP)	3.15	no	1DS5	[15]

*In these cases the status of the respective C-terminus is unclear. The indicated C-termini were not introduced genetically but presumably formed by spontaneous degradation.

amount of local disorder and the care during the structure refinement-features of the initial model. In particular, in the case of low-resolution (around 3 Å) molecular replacement structures, the expert advice that one 'should be very cautious and suspicious of the results' [26] should be taken seriously.

A model bias can be avoided by solving a structure *ab initio* as was done among the CK2 structures only for the first CK2β structure [7]. This fact together with good resolution (1.74 Å) gives the structure of *hs*CK2β$^{1-182}$ [7] the rank of a technical reference structure for CK2β. In a functional sense the missing C-terminal segment certainly limits its value; hence, the recently published structure of *hs*CK2β$^{1-193}$ – a construct that is fully competent for CK2α-binding – is a useful supplement [27].

Since no *ab initio* structure of CK2α exists so far, we solved such a structure for this review using an X-ray diffraction data set with optimized anomalous signal (see Raaf et al. [28] for details). We submitted these data to the AutoRigshaw server [29], selected the SAS protocol ('single anomalous scattering on the basis of sulphur') and thus determined initial phases of the diffracted beams. These phases were then combined with the corresponding high-resolution structure factor amplitudes [30] and served as a basis for automated [31] and finally manual [20] model building. The final structure (PDB code 3H30) represents a technical reference structure for CK2α. In the PDB it replaces its molecular replacement based pendant 2RKP [30]. Some interesting differences between both structures will be described elsewhere.

As in the case of CK2β, the technical reference structure of CK2α is not identical with the functional one since the former contains the ATP-binding region in a conformation that is not fully productive. We will show this below, and we will introduce instead the structure of maize CK2α in complex with an ATP analogue (PDB code 1LP4) [32, 33] as the most relevant CK2α structure in a functional sense. Finally, for the CK2 holoenzyme, the predominant carrier of CK2 activity in higher animals, a functionally important structure exists [8], but its technical limitations make a high-resolution update – preferably solved with an *ab initio* technique – highly desirable.

Global structural comparisons – detection of variable and invariable regions

Enzymes require structurally invariable frameworks for their function as well as adaptable regions. EPKs in particular are typically regulatable enzymes and exploit a considerable plasticity in some key regions for activity control [47]. Global structural comparisons can reveal such regions and distinguish them from rigid zones. We performed such analyses here in a way that reduced the impact of crystal packing and refinement errors and the statistical significance of the results improved. First we included only backbone atoms in the calculations, and second, we took all available protomers rather than selecting single representatives. Such a comprehensive approach is suggested by a recent analysis of the solution dynamics of ubiquitin in which an ensemble of conformers was detected, covering all 46 ubiquitin crystal structures available at that time [48]. In other words: the collectivity of all crystal structures of a protein is an approximation of its solution state. The PDB files listed in Table 1 contain 32 subunits of maize CK2α, 14 chains of mammalian CK2α and 16 chains of vertebrate CK2β. For each of these groups we calculated all possible pairwise structural 3D fits – 91 for mammalian CK2α, 496 for *zm*CK2α and 120 for CK2β – using all main-chain atoms for least-squares minimization. Afterwards we computed for each sequence position the mean value of the corresponding RMS deviations and plotted them versus the sequence positions (Fig. 3). Average values over the whole sequences – see horizontal lines in Figure 3 – allow a distinction of conformationally adaptable regions from rigid ones.

We performed a similar analysis for CDK2, a close CK2α relative from the CMGC family of EPKs (Fig. 3C). In this case nearly 15 000 pairwise 3D fits were included. A comparison of Figure 3A, B with Figure 3C shows that CK2α is significantly more rigid than CDK2 (note the different scales on the y-axes). In particular, maize CK2α (Fig. 3B) obtains an extremely narrow conformational space, while mammalian CK2α (Fig. 3A) shows some interesting local flexibilities to be addressed later.

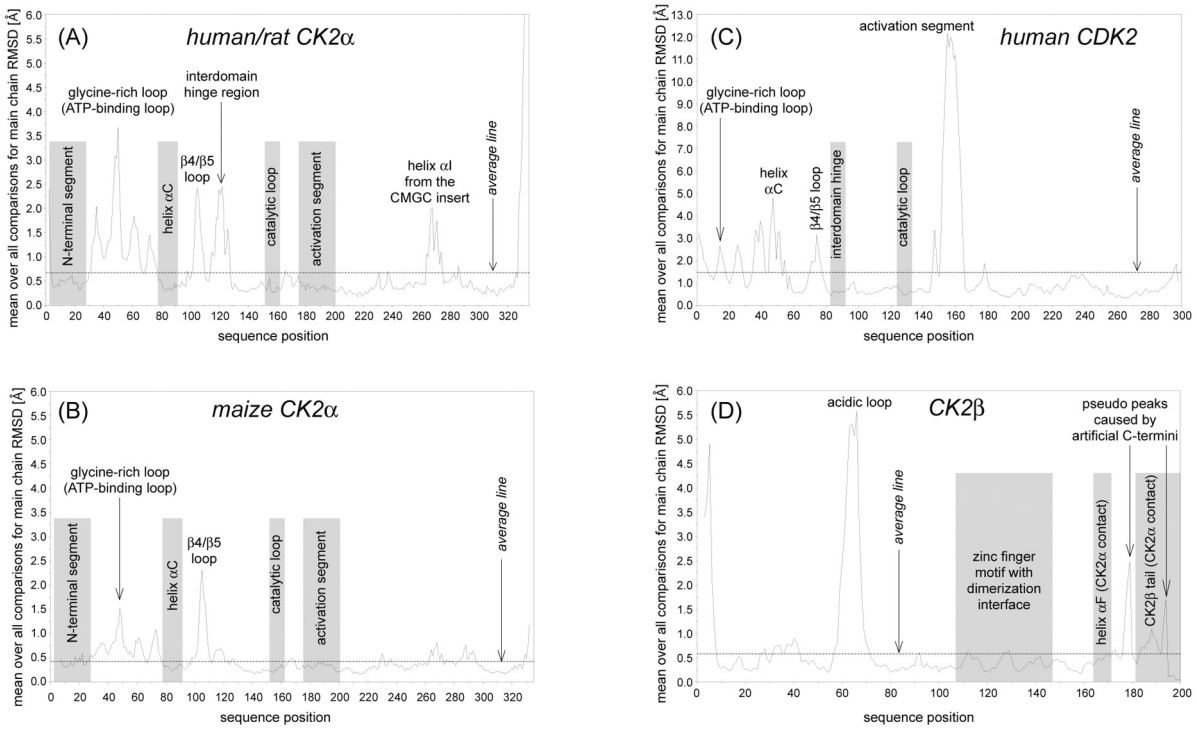

Figure 3. Comprehensive conformational analysis of CK2 and CDK2 crystal structures. All possible pairwise 3D fits within four clusters of structures – mammalian CK2α (*A*), maize CK2α (*B*), human CDK2 (*C*) and CK2β (*D*) – were calculated with the program LSQKAB [49], including all main-chain atoms. For each residue the least-squares-minimized RMS deviations were averaged over all four non-hydrogen main-chain atoms. The resulting mean values were again averaged over all 3D fits within the respective cluster of structures and plotted against the sequences. A horizontal line in the height of the average over the whole sequence supports the distinction of adaptable from invariable regions. Several rigid zones are indicated by grey patches.

In general the terminal residues of proteins are regions of enhanced flexibility unless they are particularly fixed, like the N-terminal region of CK2α (especially maize CK2α) (blue region in Fig. 1B). Therefore, the introduction of artificial termini can cause pseudo-peaks. This phenomenon can be seen around positions 180 and 193 of CK2β (Fig. 3D). The corresponding maxima originate from the fact that many of the CK2β structures in the PDB were solved with C-terminal truncation constructs ending near position 180 or at His193.

However, the majority of peaks visible in Figure 3 reveal genuine plasticities of the polypeptide backbones with potential biological significance. At least the highest of them indicate candidate regions that allow the proteins an adaptation to certain environments and functional situations. Moreover, there are zones of remarkable conformational invariance (grey shadows in Fig. 3). We will discuss the functional significance of examples from both groups in the following chapters.

Rigid regions

The zinc-binding motif (zinc finger) of CK2β

The first structure of a CK2β construct [7] simultaneously provided the first experimental confirmation that CK2β contains integral zinc ions and a corresponding zinc-binding motif which before had merely been predicted bioinformatically [50]. The central components of this zinc finger are four cysteine residues whose sulphur atoms form a perfect tetrahedral coordination shell for the metal ion (Fig. 4A). These cysteines and their distances in sequence are absolutely conserved and specific for CK2β proteins throughout the eukaryotic kingdom. The conserved character of this motif in sequence space is the pendant to its conformational invariance (Fig. 3D).

The zinc finger creates a highly efficient dimerization interface for CK2β [7] (Fig. 1D) and is thus a necessary condition for the formation of the CK2 holoenzyme [8] (Fig. 1E). Disruption of the zinc finger leads to a CK2β mutant lacking both the ability to dimerize and to coordinate CK2α [52]. Due to its mainly hydrophobic character, the region around the twofold

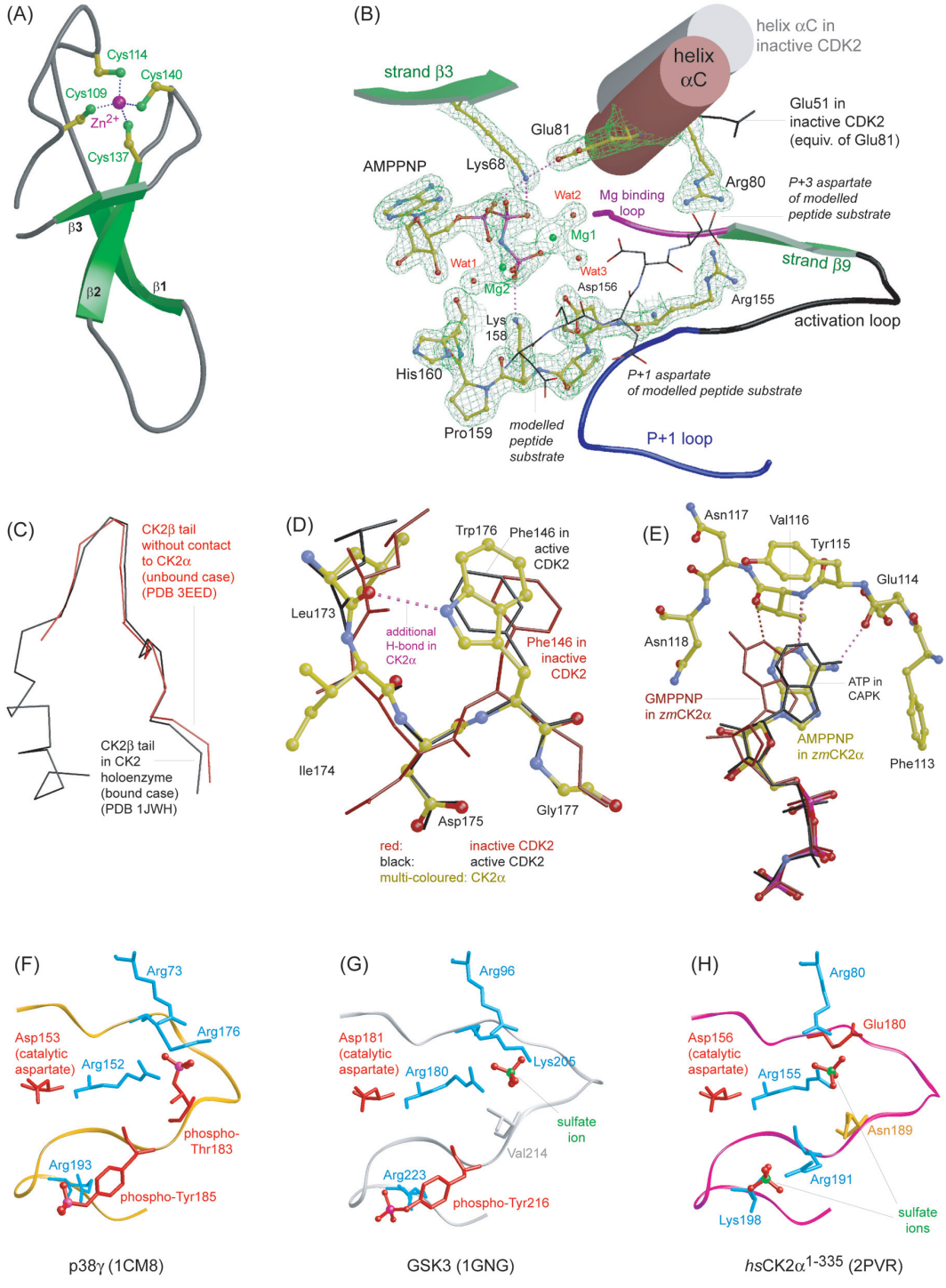

Figure 4. Rigid regions in CK2 structures. (*A*) The zinc-finger of CK2β responsible for dimerization as found in *hs*CK2β$^{1-182}$ [7]. (*B*) Catalytic key region in the complex structure of *zm*CK2α and AMPPNP [32, 33]. All important parts are well ordered, as indicated by electron density contoured at 1.5 σ. A short substrate peptide – originally modelled to *hs*CK2α$^{1-335}$ [35] – was drawn with black carbon atoms. Moreover the helix αC of inactive CDK2 [11] with the critical conserved glutamate residue is illustrated after structural superimposition. (*C*) Cα-trace of the CK2β tail region in the CK2α bound [8] and unbound [27] case. (*D*) The exceptional DWG-motif of CK2α at the N-terminal end of the activation segment. The dotted line indicates the additional hydrogen bond compared to CDK2, whose equivalent DFG motif was drawn in the active and the inactive conformation. (*E*) Structural basis of dual-cosubstrate specificity: binding of either AMPPNP or GMPPNP to the hinge region of maize CK2α. For comparison ATP as bound to CAPK [62] was drawn in black colour. (*F–H*) The anion binding sites at the activation segment filled by dual phosphorylation (p38γ; *F*), one phosphorylation and an additional sulphate ion (GSK3; G) and two sulphate ions (CK2α; H). Parts *A – E* of this figure were prepared with BOBSCRIPT [9] and Raster3D [10] and parts *f–h* with BRAGI [51].

rotation axis is a hydrophic core as normally found within single folding domains. With 540 Å^2 the interface is relatively small; as a consequence the resulting dimer is an elongated entity (Fig. 1D) with a relatively large surface in relation to its molecular weight. This qualifies CK2β ideally for its predicted role as a multivariant docking partner [53–54].

The CK2α-binding interface of CK2β

The dimerization of CK2β sets the stage for the coordination of two CK2α subunits, which is the only of the many protein/protein interactions discussed for the CK2β dimer [53–54] that has been characterized by various *in vivo* and *in vitro* methods, including protein crystallography [8], plasmon resonance [55] as well as isothermal titration and differential scanning calorimetry [27]. On the side of CK2β the necessary interface is created mainly by the helix αF and the C-terminal tail (Fig. 5A), which are rigid elements (Fig. 3D). The CK2β tail contains a small two-stranded antiparallel β-sheet (strands β4 and β5; Fig. 1C); its peptide backbone does not require the contact to CK2α for folding but is conformationally pre-formed (Fig. 4C) [27]. This is at least true up to His193, while the remaining 22 C-terminal residues of human CK2β are either only badly defined by electron density or – after Gln205 – completely disordered [8]. Calorimetric [27] and enzymological [17] experiments have shown that the residues after His193 do not contribute significantly to the affinity between CK2α and CK2β. The structure of the CK2β tail was remarkably confirmed by a recent peptide design study that resulted in effective CK2β antagonists [56].

The spatial neighbourhood of the two CK2α-binding regions does not depend on their proximity in sequence but on the dimer formation, since each of them belongs to a different CK2β subunit. The overall size of the interface established in this way is 832 Å^2 [8], which is relatively small [57] and consistent with a non-permanent character of the CK2 holoenzyme. This surprising message of the CK2 holoenzyme structure together with *in vivo* fluorescence imaging results [58] promoted 'a new view of an old molecular complex' [59], meaning that the CK2 holoenzyme might be in a dynamic equilibrium with its subunits. However, whether this is really the case under physiological conditions is an open question [60].

The catalytic loop and further key elements of catalysis in CK2α

Chemically, the selective and region-specific transfer of a high-energy phospho group from a nucleotide cosubstrate to a protein substrate is a sophisticated process [61]. Recognition, binding and spatial alignment of the two substrates – one of them after all a macromolecule – and stabilization of the transition state require several side chains and backbone regions from both main domains of the catalytic core of an EPK. Consequently, a precise spatial allocation of all these elements is a prerequisite of the reaction. It is well known that these chemical constraints enforce a high conformational similarity of active EPKs [47]. Vice versa, if only one of them is not satisfied, an inactive state results enabling very individual ways of EPK inactivation [47].

Unlike CAPK [62], CDK2 [63] and some other EPKs, no CK2α structure of a ternary complex comprising enzyme, nucleotide (plus magnesium or manganese ions) and a peptide substrate has been published so far. The best available CK2α structure to illustrate the arrangement of key residues in the centre of the active site is a binary complex of maize CK2α and AMPPNP (plus Mg^{2+} ions) [32] (Fig. 4B). (Interestingly, this complex was obtained by soaking of previously grown apo-*zm*CK2α crystals in an AMPPNP-containing solution rather than by co-crystallization. In contrast, all co-crystallization experiments with human or maize CK2α led either to nucleotide ligands with disordered or non-productively orientated triphospho moieties or – in the case of the very first *zm*CK2α structure [6] – to a complete misinterpretation of a residual electron density. The correction of this error some years later [33] is one of the rare cases in which a structure was subsequently revised by the authors.) In this structure the nucleotide, the Mg^{2+} ions and the surrounding enzyme matrix are well defined by electron density, and all these components are in equivalent positions as in the ternary complex of CAPK [62].

Several positively charged groups – two Mg^{2+} ions and the side chains of Lys68 and Lys158 – are necessary to balance the negative charge of the triphospho moiety and to align it correctly. To perform this task, Lys68 in turn requires a back stabilization by Glu81 from the helix αC (Fig. 4B). This salt bridge, whose two components are highly conserved among EPKs, is a necessary condition for and a critical identification of the active state. In inactive CDK2, for instance, it is absent because the Glu81-equivalent side chain (Glu51; black side chain in Fig. 4B) is rotated away together with the complete helix αC.

Lys158 is part of the 'catalytic loop' that ranges from Arg155 to Asn161 and is conformationally invariable in CK2α (Fig. 3A, B), in CDK2 (Fig. 3C) and in other EPKs. The central component of this loop is the 'catalytic aspartate', which is absolutely conserved among EPKs (Asp156 in CK2α; Fig. 4B). The function of this residue's side chain is the coordination of the nucleophilic hydroxy group of the substrate;

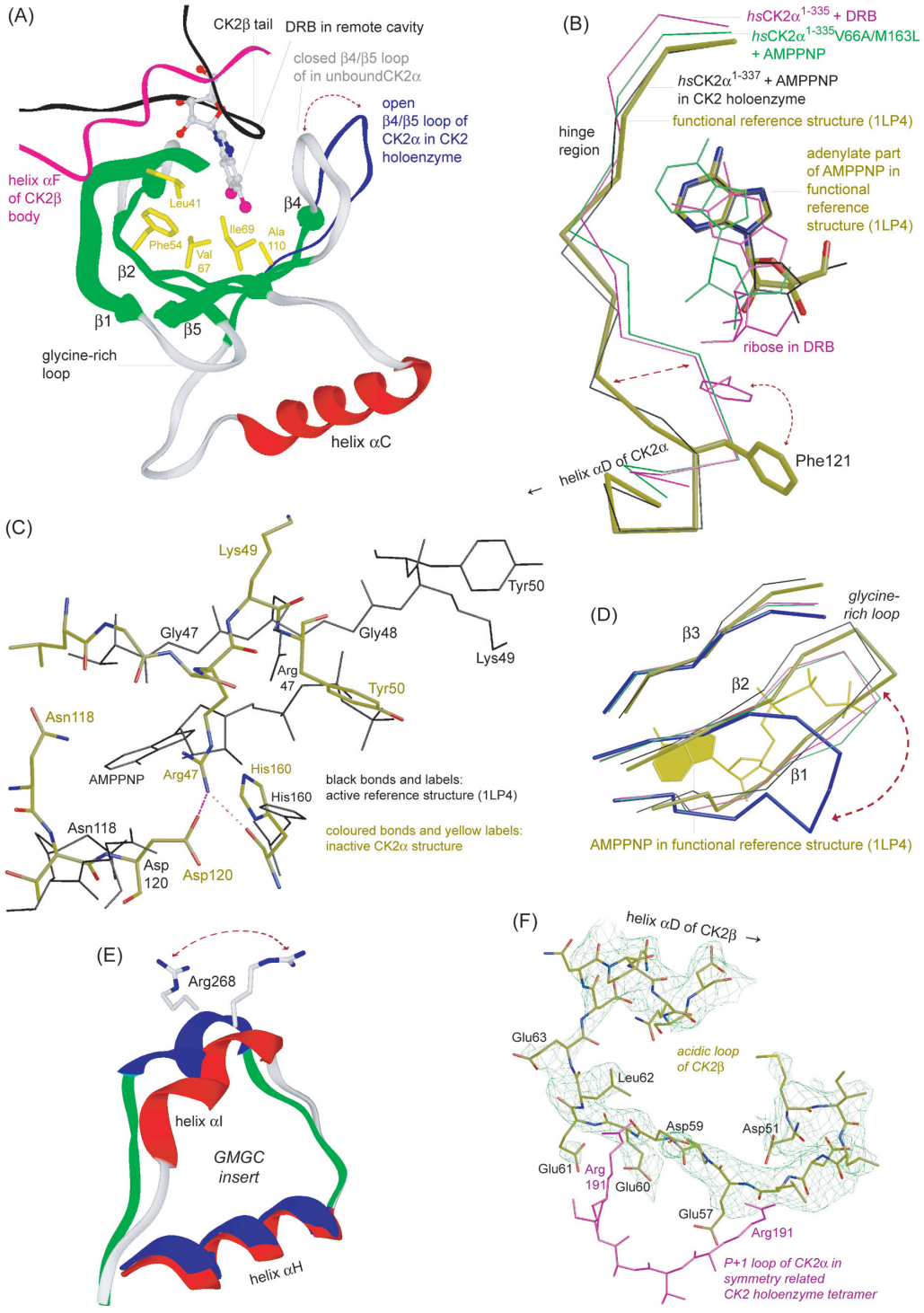

Figure 5. Dynamic regions in CK2 structures. (*A*) The β4/β5-loop of CK2α. It contributes in its open conformation (blue) to the binding interface for CK2β [8] and in its closed conformation (grey) to the remote cavity that can harbour DRB and other small molecules [30]. (*B*) The interdomain hinge region in two fundamental conformations: the open conformation is found in the functional reference structure for CK2α (*zm*CK2α/AMPPNP complex; yellow) [32] and in the CK2 holoenzyme (black) [8], while the closed conformation is represented by the *hs*CK2α$^{1-335}$/DRB complex (magenta) [30] and by the complex of *hs*CK2α$^{1-335}$V66A/M163L with AMPNP complex (green) [33]. (*C*) Collapse of the glycine-rich [42] loop changing its function from an ATP-binding element to an ATP-exclusion factor. The black bonds represent the functional reference structure (*zm*CK2α/AMPPNP) [32]. (*D*) The glycine-rich loop integrated into the antiparallel β-sheet in a view from the CK2β dimer. The colour coding is identical to panel *B* apart from the addition of a blue C_α trace showing the inactive conformation [42]. (*E*) The major part of the CMGC insert in two typical conformations found in *hs*CK2α$^{1-335}$ in complex with either DRB (red helices; [30]) or sulphate ions (blue helices; [35]). (*F*) The acidic loop of CK2β in its only partially ordered version found in chain D of the CK2 holoenzyme structure [8]. The acidic loop is covered by electron density with a contouring level of 1 σ. Panels *A* and *E* of this figure were prepared with BRAGI [51], all other parts with BOBSCRIPT [9] and Raster3D [10].

possibly it even acts as a catalytic base, abstracting the proton from the attacking group and increasing in this way its nucleophilicity [61].

Two further conserved residues (not drawn in Fig. 4B) – Asn161 and Asp175 – are required for magnesium binding and thus for stabilization of the environment of the γ-phospho group. Asp175 belongs to the 'magnesium binding loop'. According to a reasonable definition [64] the magnesium binding loop, the strand β9, the activation loop and the P+1 loop (Fig. 4B) form 'the activation segment', which is crucial for substrate binding and recognition and critically requires the correct conformation for these tasks.

Structural basis of constitutive activity

The term 'activation segment' points to a central regulatory role of this region in many EPKs [47]. As key components of cellular regulation and signal transduction, EPKs are themselves typically strictly controlled, and this control often depends on chemical modifications (phosphorylations) and conformational changes of the activation segment. The prime example for the chemical and structural basis of a stepwise protein kinase activation was provided by CDK2, which has been structurally characterized in various functional states – among them a monomeric and inactive ground form [11], a partially active form in complex with cyclin [13] and a fully active form after activation segment phosphorylation [12]. Structural comparisons of these states point to the activation segment and to the helix, αC as key elements of structural adaptation. This is illustrated in Figures 1B and 4B and is particularly emphasized by the global conformational analysis represented in Figure 3C.

In CK2α, however, these regions are invariable (Fig. 3A, B), meaning that in all CK2α structures known to date – irrespective of the species, the crystal packing, the ligands or the quarternary structure – the regulatory key elements adopt the conformations typical for active EPKs. Several structural reasons for this striking rigidity have been presented in the CK2 literature. The most important one is the extensive contact of the N-terminal segment – which is likewise conformationally invariant (Fig. 3A, B) – both to the helix αC and to the activation loop (Fig. 1B) [6]. Thus, the N-terminal segment is functionally equivalent to the cyclin A protomer in the CDK2/cyclin A complex and occupies a comparable region of space [6]. The contact region between N-terminal segment and activation segment (strictly speaking a misnomer in the case of CK2α) is further stabilized by a nearby conserved water cluster with an embedded chloride ion that was recently identified [28].

Moreover, stabilization of the activation segment in its active conformation is the most plausible explanation for a conspicuous sequence variation in the magnesium binding loop. In most EPKs this loop contains the sequence motif 'DFG', compared to 'DWG' in CK2α. The canonical magnesium binding loop with a central phenylalanine is potentially dynamic. In CDK2, for instance, the plasticity of the activation segment begins in this region and includes a rotamer change of the central phenylalanine (Fig. 4D). For the inactivation of MAP kinase this phenylalanine residue can even flip to completely different positions referred to as 'DFG-out' conformations [65, 66]. In CK2α, however, the tryptophane substituting the central phenylalanine permits an additional hydrogen bond that disfavours conformational changes (Fig. 4D).

Consistent to these structural features, the removal of the N-terminal segment results in a loss of the catalytic activity [67]. In this context it was demonstrated that CK2β can rescue the activity of these inactive deletion mutants [67]. A possible explanation for this observations is that the activation segment lacking the contact to the N-terminal segment adopts an inactive conformation but refolds to the active form in the presence of CK2β [67]. Structures of those inactive mutants have been solved neither alone nor in complex with CK2β, so that this hypothesis remains unvalidated.

The strong stabilization of the active conformation of CK2α by intermolecular constraints provides the rationale of a long-known feature of CK2 [50]: its 'constitutive activity', meaning the independence from external stimuli like (de)phosphorylation, second-messenger binding or coordination of regulatory proteins. What does this mean for the central problem of CK2 research in the last decades – the search for a regulatory mode that works under physiological conditions? The conformational invariance of the activation segment excludes regulatory modes similar to those of CDKs and MAP kinases, but it does not necessarily mean that no regulation of CK2 on the level of the protein exists at all. Glycogen synthase kinase 3 (GSK3) for instance – like CDK2 a close CK2α relative – is rigid in those regions, too, but nevertheless it can be either further stimulated by phosphorylation at the activation segment [68] or downregulated by phosphorylation of its N-terminal region [69]. Thus, also for CK2 it makes sense to look for alternative modes of regulation that do not require alterations in the canonical EPK control elements.

Structural basis of substrate recognition

One of the gaps in our structural knowledge of CK2 is the fact that the enzyme has so far not been able to be crystallized in complex with a peptide or even a protein substrate. Hence, the structural basis of the well-established fact that CK2 prefers substrates with negatively charged residues at positions P+1 and P+3 from the phosphor acceptor site (consensus sequence S/T-D/E-X-D/E) [70] has never been unambiguously clarified.

The best structure to fill this gap is based on the C-terminal truncation mutant *hs*CK2α$^{1-335}$ to which two sulphate ions were found attached at the activation segment (PDB code 2PVR [35]). Many EPKs – and especially the closest relatives of CK2α within the CMGC family – have anion binding sites in this region; these are often used for regulatory purposes [64], namely for harbouring phospho groups previously attached to a threonine and to a tyrosine phosphorylation site at the activation loop. Frequently significant structural alterations in the activation segment are required to establish these anion binding sites [64]. In other words: phosphorylation, rearrangement of the activation segment and coordination of the inserted phospho groups are concerted events.

A good example for this principle is the MAP kinase p38γ, which is phosphorylated twice in its activated form [71] and binds one of the two phospho groups at the P+1 loop and the other in a positively charged pocket at the activation loop (Fig. 4F). In GSK3 both anion binding pockets are preserved, but the threonine phosphorylation site was lost during evolution. As a consequence, in the structure of fully active GSK3, only the P+1 pocket is filled by a phospho group bound to the enzyme itself, while the second site was found to be occupied by a sulphate ion [72] (Fig. 4G). GSK3 uses this site for binding and recognition of substrates with a primed phosphorylation at the P+4 position [73].

Finally, in CK2α neither of the two phosphorylation sites is present any longer (Fig. 4H). However, as the two bound sulphate ions [35] prove, the anion binding sites are still preserved, and no structural rearrangements are required to establish them. Following the line of arguments of the GSK3 case, it is likely that CK2α uses both sites for substrate recognition, a hypothesis fitting nicely to the consensus sequence of CK2 substrates (S/T-D/E-X-D/E) [70]. Accordingly a substrate peptide with the sequence DSDDD could be plausibly modelled to *hs*CK2α$^{1-335}$ in such a way that the P+1 and the P+3 aspartate side chains coincide with the two sulphate ions [35] and that the P+3 aspartate is located near Lys77, which is consistent with previous mutational studies [74]. The model was supported by the detection of chloride ions in the relevant region, indicating binding sites for negatively charged groups [28]. For illustration we superimposed this partially modelled enzyme/substrate complex to the enzyme/cosubstrate complex visible in Fig. 4B, where the peptide substrate was drawn.

Taken together, while in the MAP kinases the anion binding sites are only formed after full activation and are exclusively used for regulatory purposes, they are pre-formed in CK2α, free from any regulatory function and pure substrate recognition sites. This finding does not only provide a plausible structural rationalization of the enzyme's substrate specificity (at least concerning the microenvironment around the phosphorylation site), it also emphasizes its exceptional constitutive activity. Therefore, it was concluded from these results [35] that CK2α probably never adopts an inactive conformation and that any control mechanism of CK2 activity should work on the level of the CK2 holoenzyme. A recently published *hs*CK2α$^{1-335}$ structure [42], however, has opened an unexpected further option described below.

The cosubstrate binding site of maize CK2α – structural basis of dual-cosubstrate specificity

The majority of functional key elements – those responsible for catalysis and substrate recognition – are conformationally invariable in CK2α (Fig. 3A, B). Yet in the case of cosubstrate binding and recognition the situation is more complicated: the most important regions for these functionalities – first the ATP-binding loop (glycine rich loop) that connects the strands β1 and β2 (Fig. 1A) and second the interdomain hinge region – are conformationally conserved in maize CK2α but more variable in human CK2α (the modest plasticity indicated in Fig. 3B for the ATP-binding loop of *zm*CK2α is largely due to one outlier, the complex structure with ATP-competitive inhibitor emodin [45]). Therefore, we introduce the basic functionality of this region here with maize CK2α and describe its local adaptability in human CK2α and the inferences of this feature later.

Nowadays, the pharmacological relevance of ATP-competitive inhibitors makes the ATP site the structurally best explored region of EPKs. This is also true for CK2, so that details of its interactions with inhibitory ligands are described in a separate part of this multi-author review [75]. However, in the case of CK2 there was a special interest in the structural details of the ATP site long before any pharmacological interest: it has been known since the 1960 s [76] that CK2 can accept GTP as a phospho donor as efficiently as ATP. The structural basis of this 'dual

cosubstrate specificity' was elucidated with two comparative complexes of *zm*CK2α with either AMPPNP or GMPPNP [32].

AMPPNP binds to *zm*CK2α similarly as ATP to CAPK (Fig. 4E): the hydrogen bonding potential of the adenine moiety is saturated equivalently, namely by two peptide groups of the interdomain hinge region (Glu114 and Val116 in the case of *zm*CK2α; Fig. 4E). For GMPPNP, however, this is impossible, since the hydrogen-bonding potential of guanine differs from that of adenine. It can only be saturated by a shift of the guanine base of GMPPNP along the peptide backbone (Fig. 4E). Interestingly, both the triphospho regions and the enzyme matrices are essentially identical in both cases. All adaptation work is left to water molecules (not drawn in Fig. 4E), which are placed as necessary to saturate the hydrogen-bonding potentials both of the enzymes and of the respective ligand. Thus, the rigidity of *zm*CK2α in the ATP-binding cleft, which is obvious from the all-against-all comparison (Fig. 3A), emerged already in the early complex structures and was particularly confirmed by an apo-structure [41] that differed only in some side chains from the binary complexes.

Figure 4E suggests that the two nucleo bases of AMPPNP and GMPPNP define a plane. Obviously, CK2α allows a certain degree of freedom within this plane for flat (parts of) ligands as long as the hydrogen-bonding pattern is preserved. The exact orientation of the plane is defined by its flanking residues Ile66 (Val66 in *hs*CK2α) and Met163. In subsequent structure-based protein design work with human CK2α, these two residues were exchanged against their equivalents in CAPK [33]. In the resulting mutant *hs*CK2α$^{1-335}$V66A/M163L, the 'adenine base binding plane' was indeed somewhat inclined as it had been predicted before. In this novel orientation the plane apparently lost its 2D freedom to a certain degree, since the original dual-cosubstrate specificity was changed to a clear preference of ATP over GTP [33].

In summary, this mutant of human CK2α confirmed the concepts about cosubstrate binding obtained on the basis of maize CK2α. Hence, at that time there was no doubt that the conspicuous rigidity of maize CK2α around the cosubstrate site was likewise a feature of the human homolog. However, in retrospect it was the structure of the *hs*CK2α$^{1-335}$V66A/M163L mutant in which for the first time a novel conformation of the interdomain hinge region was observed [33]. At first, this conformation was interpreted as a consequence of the introduced point mutations [33]; only later was it also found without these mutations and thus recognized as an inherent feature of human CK2α [30] and as a prime example for a dynamic region of the enzyme.

Dynamic regions

The β4/β5-loop of CK2α: Structural basis of CK2 holoenzyme formation and non-competitive inhibition

Before we go into the details of the particular flexibility of human CK2α in the ATP-binding region, it is necessary to describe the adaptability in the β4/β5 loop. The two regions are not in direct spatial proximity (Fig. 1A). Yet the gap between them can be filled either by CK2β [8, 16] or by certain small molecules [30] (Fig. 5A), suggesting a structural and functional correlation between the β4/β5 and the ATP-binding loop mediated via the bound ligand.

All loops connecting the β-strands in the N-terminal domain of CK2α display a somewhat enhanced plasticity as is typical for loop regions in proteins (Fig. 3A). However, the β4/β5 loop is particularly variable. This loop is part of the CK2α/CK2β interface; it adopts an extended (open) conformation in the CK2 holoenzyme [8], but a closed one, in which it is bent towards the concave surface of the β-sheet populated with hydrophobic side chains (Fig. 5A), in all existing structures of isolated human or rat CK2α irrespective of the crystallization and crystal-packing conditions.

Thus, in mammalian CK2α an unambiguous coupling of the β4/β5 loop conformation and the quarternary structure exists. In contrast, in maize CK2α both loop conformations also occur but without a clear biochemical background, so that in this case the less frequent closed conformation was interpreted as an exceptional artifact of crystal dehydration [38].

Since the closed β4/β5 loop conformation is spatially incompatible with the binding of CK2β (Fig. 5A), an opening of the loop is a necessary condition for the CK2 holoenzyme formation. It was even argued [27] that this conformational change – which is particularly conspicuous in comparison to the aforementioned rigidity of the CK2β part of the CK2α/CK2β interface – might be a driving force for the high affinity between CK2α and CK2β (dissociation constant 12.6 nM [27]). This hypothesis is unproven so far, but its background was the observation that the standard free enthalpy of the subunit interaction is mainly contributed by the enthalpy rather than the entropy.

While the β4/β5 loop in its open conformation enables CK2β binding, in its closed conformation it is part of a (partly) hydrophobic cavity. This cavity can act as an alternative binding site for certain ATP-competitive inhibitors such as DRB (Fig. 5A), and was therefore termed 'remote cavity' [42] in contrast to the canconical ATP site. The binding of DRB to the remote cavity has an inhibitory impact on CK2α, which can be enzymologically distinguished from the ATP-compet-

itive effect of DRB [30] and which is absent if the cavity is impaired and blocked by CK2β. It is possible that some recently described non-ATP-competitive inhibitors that were originally discovered as substances to disturb the CK2α/CK2β interaction [77] are also bound to the remote cavity because CK2β removes their inhibitory effect and obviously displaces them from their binding site. Apart from synthetic small molecules natural metabolites can occupy the remote cavity. This was shown for glycerol [30, 42] and for acetate ions [K. Niefind, unpublished results], both of which overlap with the flat benzimidazole moiety of DRB.

In summary, the remote cavity is a relatively unspecific binding site at the N-terminal domain of human CK2α formed in the absence of CK2β by the closed β4/β5 loop and the hydrophobic surface of the antiparallel β-sheet. It can be occupied by small molecules, and this occupation can change the activity of the enzyme or even the oligomerization state. All this suggests a further exploration of the remote cavity and its constituting elements.

Plasticity in the cosubstrate binding region of human CK2α: A key for CK2 regulation?

In the first structures of human CK2α in CK2β-bound [8] and in unbound form [44], the two main regions responsible for ATP-binding – the glycine-rich loop and the interdomain hinge – were essentially similarly folded as in maize CK2α. In particular, the CK2 holoenzyme structure [8], in which two functional states of the ATP-binding site were captured, apparently confirmed the impression of a vastly rigid catalytic subunit: one of the CK2α subunits contains an AMPPNP ligand, while the other one is in the apo-state. But despite this difference only small adaptations of the enzyme occur. Moreover the adenine and the ribose part of the AMPPNP ligand are in similar positions, as in the functional reference structure for CK2α (Fig. 5B).

As denoted above the situation changed with the structure of the mutant *hs*CK2α$^{1-335}$V66A/M163L in complex with AMPPNP [33]. In this and some subsequent structures of human and rat CK2α, an alternative conformation of the interdomain region was detected so that this region is now among the most adaptable ones (Fig. 3A). In a cluster analysis the set of human CK2α structures was divided into those with an open (and *zm*CK2α-similar) hinge region and those with a closed one [34]. Both principle conformations of this region are visible in Figure 5B with two representatives. Particularly conspicuous is the conformational change of Phe121, which resembles the switch between 'DFG-in' and 'DFG-out' in the MAP kinase p38γ [66]: in the closed conformation the Phe121 side chain points to the interior of the CK2α, but in the open one to the surface.

What consequences does the closure of the hinge region have for ATP binding? On the one hand access to the binding cavity is not prohibited, since both in the complex of *hs*CK2α$^{1-335}$V66A/M163L with AMPPNP [33] and in the *hs*CK2α$^{1-335}$/DRB complex [30] the ATP site is occupied (Fig. 5B). However, a comparison with the *zm*CK2α/AMPPNP complex [32] suggests that the closed hinge region conformation corresponds to a non-productive mode of nucleotide binding since already the position of the nucleotide ribose (and even more that of the triphospho moiety) is far away from the functional state (Fig. 5B).

Hence CK2α with a closed conformation of the hinge region may represent a partly inactive state of the enzyme. This assumption is supported by a recent structure in which not only the hinge region but also the glycine-rich loop was strongly changed (Fig. 5C, D) and had moved into the ATP site (Fig. 5C) [42]. The crystals for this structure had been grown in the presence of AMPPNP and Mg^{2+} ions, but nevertheless no nucleotide was bound. Rather, the side chain of Arg47 crosses the ATP-binding cleft, establishes a contact to Asp120 and overlaps with the canonical ribose region of the ATP site (Fig. 5C).

Thus, by a conformational transition the glycine-rich loop changed from an ATP-binding to an ATP-exclusion element. The resulting CK2α structure is the first one, for which the characterization 'inactive' is justified. Significantly the conserved ion pair typical for active EPKs (Lys68 and Glu81 in CK2α; Fig. 4B) is no longer present since Lys68 has obtained Asp175 – the magnesium binding aspartate of the active conformation – as an alternative salt bridge partner.

It should be noted that this is a real 'conformation' in a chemical sense, i.e. unlike MAP kinases and other EPKs no covalent modification like (de-)phosphorylation is required for the transition between active and inactive forms. Therefore, it is reasonable to assume a conformational equilibrium in solution as indicated in Figure 6 and to ask which factors may affect this equilibrium.

Possible candidates to support the inactive conformation are small molecules. In the corresponding crystal structure [42] the remote cavity is filled with glycerol, but glycerol itself is no inhibitor of CK2α so that this occupation is certainly not sufficient to promote the inactive conformation. However, other small molecules – like the non-ATP-competitive inhibitors mentioned above [77] – may be more effective (Fig. 6). Thus, it is possible that CK2β-free populations of CK2α whose existence has been reported [78]

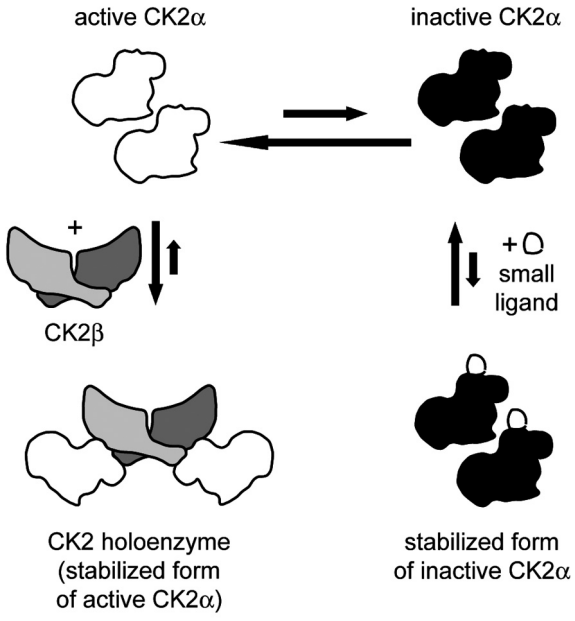

Figure 6. A hypothetical working model for CK2α regulation. According to the conformational selection model of protein interactions [79] CK2β stabilizes the active conformation but certain small molecules support the inactive conformation of CK2α. The figure is adapted from Raaf et al. [42].

contain inactive conformations of the enzyme in significant amounts.

In contrast to the favouring effects, at least one disfavouring factor of the inactive conformation is less speculative: CK2β stabilizes the whole β-sheet, including the glycine-rich loop from the distal side (Fig. 5A), so that its collapse into the ATP-binding site is prohibited. In the sense of the recently reported [48] conformational selection model of protein/protein interactions [79] this means that while (at least) human CK2α exists in solution as an ensemble of active and (partially) inactive conformers and is thus not fully competent for catalysis, CK2β specifically selects and stabilizes the fully active one (Fig. 6). This model may provide for the first time a plausible structural basis of CK2α stimulation by CK2β. It will be a proof of this model and an attractive task in the future to identify small molecules or other factors that shift the assumed conformational equilibrium to the inactive side (Fig. 6).

The CMGC-insert of CK2α – a region relevant for substrate recognition?

The helical insert in the C-terminal domain (Fig. 1A) is a typical but functionally somewhat mysterious feature of the CMGC family of EPKs [14]. For structural stability of the C-terminal domain this region is superfluous, but its existence and conservation indicate a functional relevance. A plausible structure/function correlation for the CMGC insert was shown only for the MAP kinase ERK2 [80] where the CMGC insert can fold in such a way that it stabilizes an inactive conformation of the activation segment.

Moreover it was speculated that the CMGC insert might play a role for substrate docking [14]. In fact, in recent years the spatial separation of catalytic function from recognition of substrate proteins has attracted increasing attention in EPK research [81]. It is clear now that the integration of EPKs in complex regulatory networks requires more sophisticated mechanisms of molecular recognition than is possible with the close-up range around the active site. While many EPKs have special targeting domains to recognize protein interaction partners, CMGC kinases favour an alternative strategy [81]: they dispose of special docking sites located preferentially on the kinase itself as in the MAP kinase ERK2 [82] or on interaction partners as in the case of CDK/cyclin complexes [83].

The CMGC insert of CK2α is probably no remote docking site in a strict sense, i.e. there are no indications so far that it recognizes special sequence patterns. Nevertheless it may have subtle positive or negative effects on various CK2 substrates and thus favour or disfavour some of them. The adaptability shown at least by human CK2α (Fig. 3A; Fig. 5E) is probably helpful in this context. At any rate it helps the enzyme to form different crystal packings which represent a special form of protein/protein interactions.

The puzzling acidic loop of CK2β – a trigger for aggregation?

Finally the acidic loop of CK2β with a high negative charge density deserves a note among the dynamic regions of the CK2 subunits (Fig. 3D). 'Flexibility' means disorder in this region; it is so high that – with one exception – each of the available structures is interrupted somewhere within the loop. The only exception is one of the CK2β chains of the CK2 holoenzyme structure [8], but even there the degree of disorder results in an electron density of such low quality that only a coarse backbone tracing is possible (Fig. 5F).

The very limited order in the region depends on protein/protein interactions imposed by the local environment within the CK2 holoenzyme crystals. Among others, the acidic loop touches the P+1 loop of a CK2α chain belonging to a symmetry-releated CK2 holoenzyme tetramer (Fig. 5F). This structural detail fits to various

data and observations with the CK2 holoenzyme [84], in particular its tendency to reversibly form higher-order aggregates. Since this aggregation is coupled to an inactivation, it was speculated that it might play a significant role for CK2 regulation [84]. It was never definitely proven so far that such CK2 holoenzyme aggregates exist *in vivo*, but at least a strong indication was provided: *in vitro* the aggregation of CK2 holoenzyme tetramers was shown to be correlated to their autophosphorylation, more precisely to *trans*-phosphorylation of CK2β [85, 86], and since CK2 autophosphorylation was indeed detected in cells [87], aggregation should also exist *in vivo*. At any rate, the CK2 holoenzyme crystals show that a suitable molecular environment can impose a partial order in the acidic loop of CK2β. Vice versa, the acidic loop supports in this way the docking of the CK2 holoenzyme to other molecules or to molecular ensembles.

Conclusions

With the initial key structures of CK2 entities (Fig. 1) the fundamental structure/function correlations having to do with this remarkable enzyme seemed to be comprehensively elucidated. Consequently, follow-up work on CK2 structures was primarily application-orientated, i. e. to support the important goal of developing effective and selective inhibitors for pharmacology and chemical biology. Only recently, novel structures have indicated that the conformational space of the enzyme is larger than assumed and in particular includes inactive conformations (Fig. 6). These findings raise many new questions and may thus open a new round of CK2 structural biology in the future.

Acknowledgement. This work was supported by the Danish Research Council (grant 21-01-0511 to O.G.I.) and by the Deutsche Forschungsgemeinschaft (DFG; grant NI 643/1–3 to K.N.I.).

1 Knighton, D. R., Zheng, J., Ten Eyck, L. F., Ashford, V. A., Xuong, N. H., Taylor, S. S. and Sowadski, J. M. (1991) Crystal structure of the catalytic subunit of cyclic adenosine monophosphate-dependent protein kinase. Science 253, 407–414.
2 Hanks, S. K. and Hunter, T. (1995) Protein kinases 6. The eukaryotic protein kinase superfamily: kinase (catalytic) domain structure and classification. FASEB J. 9, 576–596.
3 Sarno, S., Vaglio, P., Cesaro, L., Marin, O. and Pinna, L. A. (1999) A multifunctional network of basic residues confers unique properties to protein kinase CK2. Mol. Cell. Biochem. 191, 13–19.
4 Dobrowolska, G., Meggio, F., Marin, O., Lozeman, F. J., Li, D., Pinna, L. A. and Krebs, E. G. (1994) Substrate recognition by casein kinase-II: the role of histidine-160. FEBS Lett. 355, 237–241.
5 Sarno, S., Vaglio, P., Marin, O., Issinger, O.-G., Ruffato, K. and Pinna, L. A. (1997) Mutational analysis of residues implicated in the interaction between protein kinase CK2 and peptide substrates. Biochemistry 36, 11717–11724.
6 Niefind, K., Guerra, B., Pinna, L. A., Issinger, O.-G. and Schomburg, D. (1998) Crystal structure of the catalytic subunit of protein kinase CK2 from *Zea mays* at 2.1 Å resolution. EMBO J. 17, 2451–2462.
7 Chantalat, L., Leroy, D., Filhol, O., Nueda, A., Benitez, M. J., Chambaz, E. M., Cochet, C. and Dideberg, O. (1999) Crystal structure of the human protein kinase CK2 regulatory subunit reveals its zinc finger-mediated dimerization. EMBO J. 18, 2930–2940.
8 Niefind, K., Guerra, B., Ermakowa, I. and Issinger, O.-G. (2001) Crystal structure of human protein kinase CK2: insights into basic properties of the CK2 holoenzyme. EMBO J. 20, 5320–5331.
9 Esnouf, R. M. (1997) An extensively modified version of MolScript that includes greatly enhanced coloring capabilities. J. Mol. Graph. 15, 132–134.
10 Merritt, E. A. and Bacon, D. J. (1997) Raster3D: photorealistic molecular graphics. Methods Enzymol. 277, 505–524.
11 De Bondt, H. L., Rosenblatt, J., Jancarik, J., Jones, H. D., Morgan, D. O. and Kim, S.-H. (1993) Crystal structure of cyclin-dependent kinase 2. Nature 363, 595–602.
12 Russo, A. A., Jeffrey, P. D. and Pavletich, N. P. (1996) Structural basis of cyclin-dependent kinase activation by phosphorylation. Nat. Struct. Biol. 3, 696–700.
13 Jeffrey, P. D., Russo, A. A., Polyak, K., Gibbs, E., Hurwitz, J., Massague, J. and Pavletich, N. P. (1995) Mechanism of CDK activation revealed by the structure of a cyclinA-CDK2 complex. Nature 376, 313–320.
14 Kannan, N. and Neuwald, A. F. (2004) Evolutionary constraints associated with functional specificity of the CMGC protein kinases MAPK, CDK, GSK, SRPK, DYRK, and CK2α. Protein Sci. 13, 2059–2077.
15 Qian, X., Gozani, S. N., Yoon, H., Jeon, C. J., Agarwal, K. and Weiss, M. A. (1993) Novel zinc finger motif in the basal transcriptional machinery: three-dimensional NMR studies of the nucleic acid binding domain of transcriptional elongation factor TFIIS. Biochemistry 32, 9944–9959.
16 Battistutta, R., Sarno, S., De Moliner, E., Marin, O., Issinger, O.-G., Zanotti, G. and Pinna, L. A. (2000) The crystal structure of the complex of *Zea mays* α subunit with a fragment of human β subunit provides the clue to the architecture of protein kinase CK2 holoenzyme. Eur. J. Biochem. 267, 5184–5190.
17 Boldyreff, B., Meggio, F., Pinna, L. A. and Issinger, O.-G. (1993) Reconstitution of normal and hyperactivated forms of casein kinase-2 by variably mutated β-subunits. Biochemistry 32, 12672–12677.
18 Berman, H. M., Westbrook, J., Feng, Z., Gilliland, G., Bhat, T. N., Weissig, H., Shindyalov, I. N. and Bourne, P. E. (2000). The Protein Data Bank. Nucleic Acids Res. 28, 235–242.
19 Hooft, R. W. W., Vriend, G., Sander, C. and Abola, E. E. (1996) Errors in protein structures. Nature 381, 272.
20 Emsley, P. and Cowtan, K. (2004) Coot: model-building tools for molecular graphics. Acta Crystallogr. D60, 2126–2132.
21 Joosten, R. P and Vriend, G. (2007) PDB improvement starts with data deposition. Science 317, 195–196.
22 Kleywegt, G. J. (2007). Quality control and validation. Methods Mol. Biol. 364, 255–272.
23 Pagano, M. A., Cesaro, L., Meggio, F. and Pinna, L. A. (2006). Protein kinase CK2: a newcomer in the 'druggable kinome'. Biochem. Soc. Trans. 34, 1303–1306.
24 Guerra, B. and Issinger, O.-G. (2008) Protein kinase CK2 in human diseases. Curr. Med. Chem. 15, 1870–1886.
25 Nie, Z., Perretta, C., Erickson, P., Margosiak, S., Almassy, R., Lu, J., Averill, A., Yager, K. M., Chu, S. (2007) Structure-based design, synthesis, and study of pyrazolo[1,5-a][1,3,5]triazine derivatives as potent inhibitors of protein kinase CK2. Bioorg. Med. Chem. Lett. 17, 4191–4195.
26 Evans, P. and McCoy A. (2008). An introduction to molecular replacement. Acta Crystallogr D64, 1-–10.
27 Raaf, J., Brunstein, E., Issinger, O.-G. and Niefind, K. (2008) The interaction of CK2α and CK2β, the subunits of protein

kinase CK2, requires CK2β in a pre-formed conformation and is enthalpically driven. Protein Sci. 17, 2180–2186.
28 Raaf, J., Issinger, O.-G. and Niefind, K. (2008) Insights from soft X-rays: the chlorine and sulfur sub-structures of a CK2α/DRB complex. Mol. Cell. Biochem. 316, 15–23.
29 Panjikar, S., Parthasarathy, V., Lamzin, V. S., Weiss, M. S. and Tucker, P. A. (2005) Auto-Rickshaw – an automated crystal structure determination platform as an efficient tool for the validation of an X-ray diffraction experiment. Acta Crystallogr. D61, 449–457.
30 Raaf, J., Brunstein, E., Issinger, O.-G. and Niefind, K. (2008) The CK2α/CK2β interface of human protein kinase CK2 harbors a binding pocket for small molecules. Chem. Biol. 15, 111–117.
31 Perrakis, A., Morris, R. M. and Lamzin, V. S. (1999) Automated protein model building combined with iterative structure refinement. Nat. Struct. Biol. 6, 458–463.
32 Niefind, K., Pütter, M., Guerra, B., Issinger, O.-G. and Schomburg, D. (1999) GTP plus water mimic ATP in the active site of protein kinase CK2. Nat. Struct. Biol. 6, 1100–1103.
33 Yde, C. W., Ermakova, I., Issinger, O.-G. and Niefind, K. (2005) Inclining the purine base binding plane in protein kinase CK2 by exchanging the flanking side-chains generates a preference for ATP as a cosubstrate. J. Mol. Biol. 347, 399–414.
34 Raaf, J., Klopffleisch, K., Issinger, O.-G. and Niefind, K. (2008) The catalytic subunit of human protein kinase CK2 structurally deviates from its maize homologue in complex with the nucleotide competitive inhibitor emodin. J. Mol. Biol. 377, 1–8.
35 Niefind, K., Yde, C. W., Ermakova, I. and Issinger, O.-G. (2007) Evolved to be active: sulfate ions define substrate recognition sites of CK2α and emphasise its exceptional role within the CMGC family of eukaryotic protein kinases. J. Mol. Biol. 370, 427–438.
36 Sarno, S., de Moliner, E., Ruzzene, M., Pagano, M. A., Battistutta, R., Bain, J., Fabbro, D., Schoepfer, J., Elliott, M., Furet, P., Meggio, F. et al. (2003) Biochemical and three-dimensional-structural study of the specific inhibition of protein kinase CK2 by [5-oxo-5,6-dihydroindolo-(1,2-a)quinazolin-7-yl]acetic acid (IQA). Biochem. J. 374, 639–646.
37 De Moliner, E., Moro, S., Sarno, S., Zagotto, G., Zanotti, G., Pinna, L. A. and Battistutta, R. (2003) Inhibition of protein kinase CK2 by anthraquinone-related compounds. A structural insight. J. Biol. Chem. 278, 1831–1836.
38 Battistutta, R., Mazzorana, M., Sarno, S., Kazimierczuk, Z., Zanotti, G. and Pinna, L. A. (2005) Inspecting the structure-activity relationship of protein kinase CK2 inhibitors derived from tetrabromo-benzimidazole. Chem. Biol. 12, 1211–1219.
39 Battistutta, R., Mazzorana, M., Cendron, L., Bortolato, A., Sarno, S., Kazimierczuk, Z., Zanotti, G., Moro, S. and Pinna, L. A. (2007) The ATP-binding site of protein kinase CK2 holds a positive electrostatic area and conserved water molecules. Chembiochem 8, 1804–1809.
40 Chilin, A., Battistutta, R., Bortolato, A., Cozza, G., Zanatta, S., Poletto, G., Mazzorana, M., Zagotto, G., Uriarte, E., Guiotto, A. et al. (2008) Coumarin as attractive casein kinase 2 (CK2) inhibitor scaffold: an integrate approach to elucidate the putative binding motif and explain structure-activity relationships. J. Med. Chem. 51, 752–759.
41 Battistutta, R., De Moliner, E., Sarno, S., Zanotti, G. and Pinna, L. A. (2001) Structural features underlying selective inhibition of protein kinase CK2 by ATP site-directed tetrabromo-2-benzotriazole. Protein Sci. 10, 2200–2206.
42 Raaf, J., Issinger, O.-G. and Niefind, K. (2009) First inactive conformation of CK2α, the catalytic subunit of protein kinase CK2. J. Mol. Biol. 386, 1212–1221.
43 Pechkova, E., Zanotti, G. and Nicolini, C. (2003) Three-dimensional atomic structure of a catalytic subunit mutant of human protein kinase CK2. Acta Crystallogr. D59, 2133–2139.
44 Ermakova, I., Boldyreff, B., Issinger, O.-G. and Niefind, K. (2003) Crystal structure of a C-terminal deletion mutant of human protein kinase CK2 catalytic subunit. J. Mol. Biol. 330, 925–934.
45 Battistutta, R., Sarno, S., De Moliner, E., Papinutto, E., Zanotti, G. and Pinna, L. A. (2000) The replacement of ATP by the competitive inhibitor emodin induces conformational modifications in the catalytic site of protein kinase CK2. J. Biol. Chem. 275, 29618–29622.
46 Bertrand, L., Sayed, M. F., Pei, X. Y., Parisini, E., Dhanaraj, V., Bolanos-Garcia, V. M., Allende, J. E. and Blundell, T. L. (2004). Structure of the regulatory subunit of CK2 in the presence of a p21WAF1 peptide demonstrates flexibility of the acidic loop. Acta Crystallogr. D60, 1698–1704.
47 Huse, M. and Kuriyan, J. (2002) The conformational plasticity of protein kinases. Cell 109, 275–282.
48 Lange, O. F., Lakomek, N.-A., Farès, C., Schröder, G. F., Walter, K. F. A., Becker, S., Meiler, J., Grubmüller, H., Griesinger, C. and de Groot, B. L. (2008) Recognition dynamics up to microseconds revealed from an RDC-derived ubiquitin ensemble in solution. Science 320, 1471–1475.
49 Collaborative Computational Project, Number 4 (1994) The CCP4 suite: programs for protein crystallography. Acta Crystallogr. D50, 760–763.
50 Allende, C. C. and Allende, J. E. (1995) Protein kinase CK2: an enzyme with multiple substrates and a puzzling regulation. FASEB J. 9, 313–323.
51 Reichelt, J., Dieterich, G., Kvesic, M., Schomburg, D. and Heinz, D. W. (2005) BRAGI: linking and visualization of database information in a 3D viewer and modeling tool. Bioinformatics 21, 1291–1293.
52 Canton, D. A., Zhang, C. and Litchfield, D. W. (2001) Assembly of protein kinase CK2: investigation of complex formation between catalytic and regulatory subunits using a zinc-finger-deficient mutant of CK2β. Biochem. J. 358, 87–94.
53 Bibby, A. C. and Litchfield, D. W. (2005) The multiple personalities of the regulatory subunit of protein kinase CK2: CK2 dependent and CK2 independent roles reveal a secret identity for CK2β. Int. J. Biol. Sci. 1, 67–79.
54 Arrigoni, G., Pagano, M. A., Sarno, S., Cesaro, L., James, P. and Pinna, L. A. (2008) Mass spectrometry analysis of a protein kinase CK2β subunit interactome isolated from mouse brain by affinity chromatography. J. Proteome Res. 7, 990–1000.
55 Martel, V., Filhol, O., Nueda, A. and Cochet, C. (2002) Dynamic localization/association of protein kinase CK2 subunits in living cells: a role in its cellular regulation? Ann. N. Y. Acad. Sci. 973, 272–277.
56 Laudet, B., Barette, C., Dulery, V., Renaudet, O., Dumy, P., Metz, A., Prudent, R., Deshiere, A., Dideberg, O., Filhol, O. et al. (2007). Structure-based design of small peptide inhibitors of protein kinase CK2 subunit interaction. Biochem. J. 408, 363–373.
57 Jones, S. and Thornton, J. M. (1996) Principles of protein-protein interactions. Proc. Natl. Acad. Sci. USA 93, 13–20.
58 Filhol, O., Nueda, A., Martel, V., Gerber-Scokaert, D., Benitez, M. J., Souchier, C., Saoudi, Y. and Cochet, C. (2003) Live cell fluorescence imaging reveals the dynamics of protein kinase CK2 individual subunits. *Mol. Cell. Biol.* 23, 975–987.
59 Filhol, O., Martiel, J. L. and Cochet, C. (2004) Protein kinase CK2: a new view of an old molecular complex. EMBO Rep. 5, 351–355.
60 Salvi, M., Sarno, S., Marin, O., Meggio, F., Itarte, E. and Pinna, L. A. (2006) Discrimination between the activity of protein kinase CK2 holoenzyme and its catalytic subunits. FEBS Lett. 580, 3948–3952.
61 Adams, J. A. (2001) Kinetic and catalytic mechanisms of protein kinases. Chem. Rev. 101, 2271–2290.
62 Knighton, D. R., Zheng, J. H., Ten Eyck, L. F., Xuong, N. H., Taylor, S. S. and Sowadski, J. M. (1991) Structure of a peptide inhibitor bound to the catalytic subunit of cyclic adenosine monophosphate-dependent protein kinase. Science 253, 414–420.
63 Brown, N. R., Noble, M. E., Endicott, J. A. and Johnson, L. N. (1999) The structural basis for specificity of substrate and

recruitment peptides for cyclin-dependent kinases. Nat. Cell Biol. 1, 438–443.
64 Nolen, B., Taylor, S. and Ghosh, G. (2004) Regulation of protein kinases: controlling activity through activation segment conformation. Mol. Cell 15, 661–675.
65 Bukhtiyarova, M., Karpusas, M., Northrop, K., Namboodiri, H. V. and Springman, E. B. (2007) Mutagenesis of p38α MAP kinase establishes key roles of Phe169 in function and structural dynamics and reveals a novel DFG-OUT state. Biochemistry 46, 5687–5696.
66 Pargellis, C., Tong, L., Churchill, L., Cirillo, P. F., Gilmore, T., Graham, A. G., Grob, P. M., Hickey, E. R., Moss, N., Pav, S. (2002) Inhibition of p38 MAP kinase by utilizing a novel allosteric binding site. Nat. Struct. Biol. 9, 268–272.
67 Sarno, S., Ghisellini, P. and Pinna, L. A. (2002) Unique activation mechanism of protein kinase CK2: the N-terminal segment is essential for constitutive activity of the catalytic subunit but not of the holoenzyme. J. Biol. Chem. 277, 22509–22514.
68 Hughes, K., Nikolakaki, E., Plyte, S. E., Totty, N. F. and Woodgett, J. R. (1993) Modulation of the glycogen synthase kinase-3 family by tyrosine phosphorylation. EMBO J. 12, 803–808.
69 Wang, Q. M., Fiol, C. J., DePaoli-Roach, A. A. and Roach, P. J. (1994). Glycogen synthase kinase-3β is a dual specificity kinase differentially regulated by tyrosine and serine/threonine phosphorylation. J. Biol. Chem. 269, 14566–14574.
70 Meggio, F. and Pinna, L. A. (2003) One-thousand-and-one substrates of protein kinase CK2? FASEB J. 17, 349–368.
71 Bellon, S., Fitzgibbon, M. J., Fox, T., Hsiao, H. M. and Wilson, K. P (1999) The structure of phosphorylated p38γ is monomeric and reveals a conserved activation-loop conformation. Structure 7, 1057–1065.
72 Bax, B., Carter, P. S., Lewis, C., Guy, A. R., Bridges, A., Tanner, R., Pettman, G., Mannix, C., Culbert, A. A., Brown, M. J., Smith, D. G. (2001) The structure of phosphorylated GSK-3β complexed with a peptide, FRATtide, that inhibits β-catenin phosphorylation. Structure 9, 1143–1152.
73 Dajani, R., Fraser, E., Roe, S. M., Young, N., Good, V., Dale, T. C. and Pearl, L. H. (2001) Crystal structure of glycogen synthase kinase 3β: structural basis of phosphate-primed substrate specificity and autoinhibition. Cell 105, 721–732.
74 Sarno, S., Vaglio, P., Marin, O., Issinger, O.-G., Ruffato, K. and Pinna, L. A. (1997) Mutational analysis of residues implicated in the interaction between protein kinase CK2 and peptide substrates. Biochemistry 36, 11717–11724.
75 Battistutta, R. (2008) Structural bases of protein kinase CK2 inhibition. Cell. Mol. Life Sci. 66, doi 10.1007/s00018-009-9155-x.
76 Rodnight, R. and Lavin, B. E. (1964) Phosvitin kinase from brain: activation by ions and subcellular distribution. Biochem. J. 93, 84–91.
77 Laudet, B., Moucadel, V., Prudent, R., Filhol, O., Wong, Y. S., Royer, D. and Cochet C. (2008) Identification of chemical inhibitors of protein-kinase CK2 subunit interaction. Mol. Cell. Biochem. 316, 63–69.
78 Allende, C. C. and Allende, J. E. (1998). Promiscuous subunit interactions: a possible mechanism for the regulation of protein kinase CK2. J. Cell. Biochem. Suppl. 30/31, 129–136.
79 Boehr, D. D. and Wright, P. E. (2008) Biochemistry. How do proteins interact? Science 320, 1429–1430.
80 Canagarajah, B. J., Khokhlatchev, A., Cobb, M. H. and Goldsmith, E. J. (1997) Activation mechanism of the MAP kinase ERK2 by dual phosphorylation. Cell 90, 859–869.
81 Reményi, A., Good, M. C. and Lim, W. A. (2006). Docking interactions in protein kinase and phosphatase networks. Curr. Opin. Struct. Biol. 16, 676–685.
82 Zhou, T., Sun, L., Humphreys, J. and Goldsmith, E. J. (2006). Docking interactions induce exposure of activation loop in the MAP kinase ERK2. Structure 14, 1011–1019.
83 Loog, M. and Morgan, D. O. (2005) Cyclin specificity in the phosphorylation of cyclin-dependent kinase substrates. Nature 434, 104–108.
84 Niefind, K. and Issinger, O.-G. (2005) Primary and secondary interactions between CK2α and CK2β lead to ring-like structures in the crystals of the CK2 holoenzyme. Mol. Cell. Biochem. 274, 3–14.
85 Pagano, M. A., Sarno, S., Poletto, G., Cozza, G., Pinna, L. A. and Meggio, F. (2005) Autophosphorylation at the regulatory β subunit reflects the supramolecular organization of protein kinase CK2. Mol. Cell. Biochem. 274, 23–29.
86 Olsen, B. B., Boldyreff, B., Niefind, K. and Issinger, O.-G. (2006) Purification and characterization of the CK2α'-based holoenzyme, an isozyme of CK2 α: a comparative analysis. Protein Expr. Purif. 47, 651–661.
87 Litchfield, D. W., Lozeman, F. J., Cicirelli, M. F., Harrylock, M., Ericsson, L. H., Piening, C. J. and Krebs, E. G. (1991) Phosphorylation of the β subunit of casein kinase II in human A431 cells. Identification of the autophosphorylation site and a site phosphorylated by $p34^{cdc2}$. J. Biol. Chem. 266, 20380–20389.